UCRL-JC-126339
PREPRINT

Analysis of $Sr_{5-x}Ba_x(PO_4)_3F:Yb^{3+}$ crystals for improved laser performance with diode-pumping

K. I. Schaffers, A. J. Bayramian, C. D. Marshall,
J. B. Tassano, and S. A. Payne

This paper was prepared for submittal to the
12th Topical Meeting on Advanced Solid-State Lasers
Orlando, Florida
January 27-29, 1997

February 19, 1997

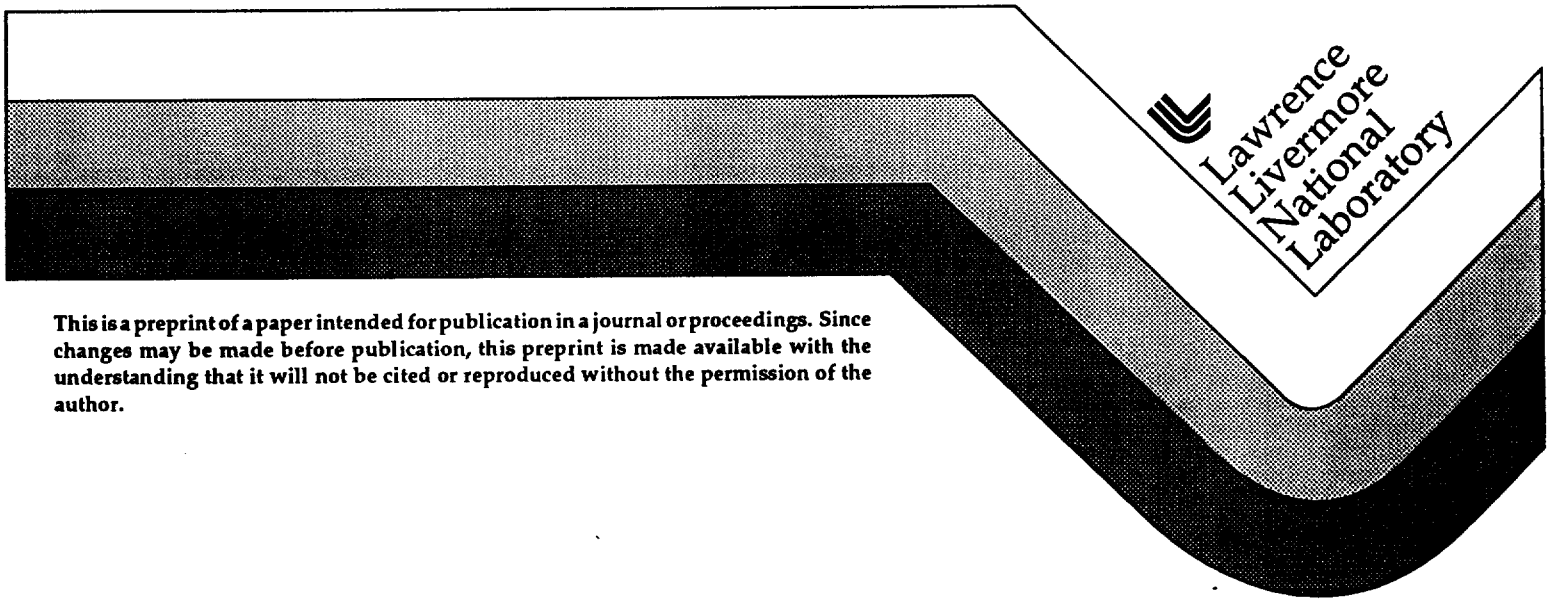

Analysis of $Sr_{5-x}Ba_x(PO_4)_3F:Yb^{3+}$ crystals for improved laser performance with diode-pumping

Kathleen I. Schaffers, Andrew J. Bayramian, Christopher D. Marshall, John B. Tassano, and Stephen A. Payne
Lawrence Livermore National Laboratory, PO Box 808, L-441, Livermore, California 94551

Abstract

Crystals of $Yb^{3+}:Sr_{5-x}Ba_x(PO_4)_3F$ ($0 \le x \le 5$) have been investigated as a means to obtain broader absorption bands than are currently available with Yb^{3+}:S-FAP [$Yb^{3+}:Sr_5(PO_4)_3F$], thereby improving diode-pumping efficiency for high peak power applications. Large diode-arrays have a FWHM pump band of ≥5 nm while the FWHM of the 900 nm absorption band for Yb:S-FAP is 5.5 nm; therefore, a significant amount of pump power can be wasted due to the nonideal overlap. Spectroscopic analysis of $Yb:Sr_{5-x}Ba_x$-FAP crystals indicates that adding barium to the lattice increases the pump band to 13-16 nm which more than compensates for the diode-array pump source without a detrimental reduction in absorption cross section. However, the emission cross section decreases by approximately half with relatively no effect on the emission lifetime. The small signal gain has also been measured and compared to the parent material Yb:S-FAP and emission cross sections have been determined by the method of reciprocity, the Füchtbauer-Ladenburg method, and small signal gain. Overall, $Yb^{3+}:Sr_{5-x}Ba_x(PO_4)_3F$ crystals appear to achieve the goal of nearly matching the favorable thermal and laser performance properties of Yb:S-FAP while having a broader absorption band to better accommodate diode pumping.

Introduction

Host materials doped with the Yb^{3+} ion have ignited a great deal of interest in the past several years for their use in solid-state lasers that can be pumped by high power InGaAs diode lasers.[1,2] These materials have approximately four times longer storage lifetimes than their Nd^{3+}-doped counterparts[3,4] allowing for greater pumping efficiency for systems employing diode lasers. In addition, the Yb^{3+} materials have a reduced quantum defect because of the relatively simple electronic structure of the Yb^{3+} ion which results in less heating of the gain media and favorable thermal performance. For example, the material and laser performance have been examined for Yb:YAG,[5] Yb:BCBF,[6] and the Yb:fluorapatite (FAP) family of crystals[7-9] including, $Ca_5(PO_4)_3F$ (C-FAP), $Sr_5(PO_4)_3F$ (S-FAP), $Ca_{5-x}Sr_x(PO_4)_3F$ (CS-FAP) and $Sr_5(VO_4)_3F$ (S-VAP)[10]. Although Yb:YAG is better for high power/high thermal load operations because of its significantly improved thermal properties, Yb:fluorapatites are especially well suited for diode pumping in high efficiency/moderate thermal load applications. The laser performance of Yb:S-FAP has recently been investigated for use in a gas-cooled-slab, diode-pumped solid-state laser (GCS DPSSL) geometry.[11] This laser was shown to produce 50 W cw of optical power at 1047 nm having a laser output efficiency of 51% with respect to absorbed pump power, where the pump source was a laser diode-array operating at 900 nm with a full-width-half-max (FWHM) of 5.5 nm. One complication that arises in constructing high power crystalline lasers of this design is the relatively narrow absorption band of ~4-6 nm in comparison with the FWHM of ≥5-10 nm for generally available, large diode-arrays used as the pump source (see for example, Figure 1).

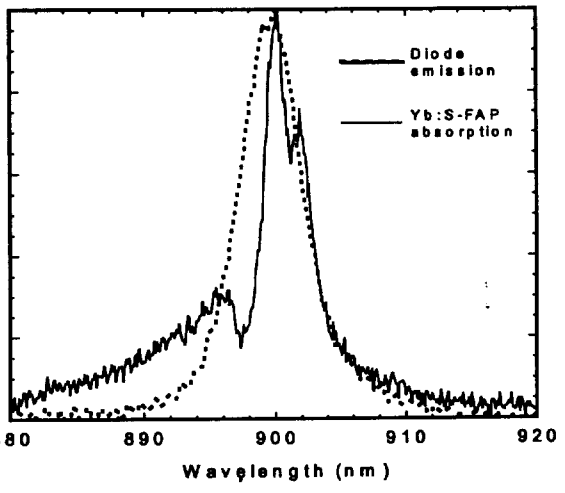

Figure 1. Overlay of a typical pulse for a large 23 kW peak power diode-array with the absorption band of Yb:S-FAP indicating a small mis-match of the bandwidths.

In essence a significant percentage of pump power is wasted because of this nonideal overlap and therefore more diode packages are needed to achieve efficient laser performance resulting in higher cost laser systems. As a result, we have been investigating a new subgroup of Yb:fluorapatite crystals that incorporate barium into the lattice, $Yb:Sr_{5-x}Ba_x(PO_4)_3F$, where the main goal was to broaden the absorption band to better accommodate diode-array performance while maintaining all other favorable laser and material properties for high peak power operation.

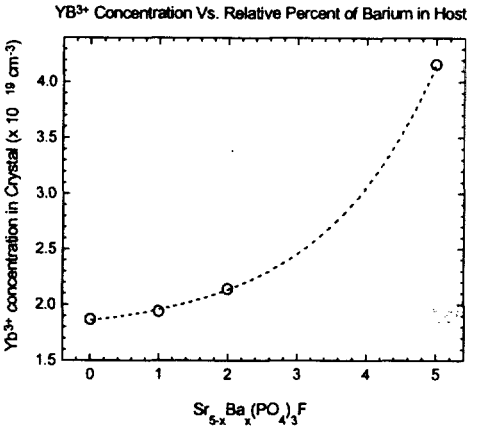

Figure 2. Plot of Yb^{3+} concentration measured for crystals of $Yb:Sr_{5-x}Ba_x(PO_4)_3F$ where $0 \leq x \leq 5$.

Crystal Growth

Crystals of $Yb:Sr_{5-x}Ba_x(PO_4)_3F$ (x = 0, 0.25, 0.5, 1, 2, 5) up to 2.8 cm diameter by 10 cm in length have been grown by using the Czochralski method. The crystals are grown in an inert atmosphere at a pull rate of 1 mm/hr and a rotation rate of 20 rpm. As-grown crystals are cloudy and therefore a post-growth annealing process has been developed to eliminate the cloudiness where the boule is suspended over the melt for up to 7 days in a temperature zone of the growth furnace that is ~300°C below the melting point.[9]

A constant starting concentration for Yb of 1 atomic percent or number density ~17 x 10^{19} cm^{-3} was maintained in the melt, $[Yb]_{melt}$, throughout the growth experiments. Yb number densities in the crystals were determined by using inductively coupled plasma and mass spectrometry techniques (ICP MS). Results indicate that the Yb distribution coefficient increases nonlinearly with Ba concentration to give number densities for $Yb:Sr_{5-x}Ba_x(PO_4)_3F$ ranging from 1.75 x $10^{19}cm^{-3}$ to 4.2 x $10^{19}cm^{-3}$ for x = 0 to x = 5, respectively (Figure 2).

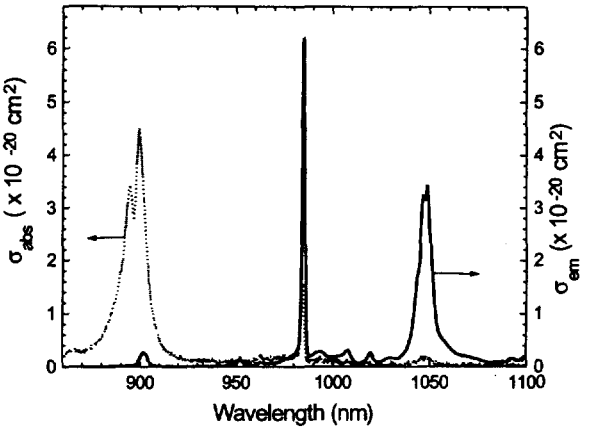

Figure 3. Sketch of the absorption and emission spectra of $Yb:Sr_4Ba$-FAP in units of absolute cross section versus wavelength.

Spectroscopy Results

Initial spectroscopic analysis of the $Yb:Sr_{5-x}Ba_x(PO_4)_3F$ (Yb:Sr,Ba-FAP) crystals appear to be favorable for achieving increased absorption bandwidth to improve diode pumping efficiency. The complete room-temperature absorption and emission spectra of the x=1, $Yb:Sr_4Ba$-FAP, material are plotted in Figure 3 on an absolute cross section scale. Diode-pumping occurs at the 900 nm absorption band and laser extraction takes place at ~1047 nm. Figure 4 displays the absorption spectra of the barium containing crystals compared to the parent Yb:S-FAP crystal, in units of absolute cross section versus wavelength. The Stark levels for Yb:S-FAP and Yb:Sr,Ba-FAP are nearly identical. It is clear that adding Ba to the $Yb:Sr_5(PO_4)_3F$ lattice significantly increases the width (FWHM) of the absorption feature from 6 nm to approximately 13 nm for $Yb:Sr_4Ba$-FAP and 16 nm for $Yb:Sr_3Ba_2$-FAP. The enhanced bandwidth for the $0 < x < 1$ crystals more than compensates for the projected 5-8 nm FWHM of the diode-array pump source without a detrimental reduction in absorption cross section. In

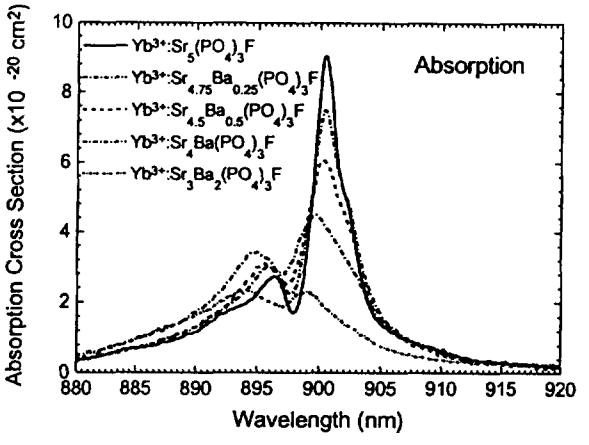

Figure 4. Absorption cross sections versus wavelength for Yb:$Sr_{5-x}Ba_x(PO_4)_3F$ crystals.

fact, there is an increase in the effective absorption cross section from ~2.8 x 10^{-20} to 3.55 x 10^{-20} cm^2 with increasing Ba content from $0 \leq x \leq 1$, for absorption from a diode bar mounted on a BeO heatsink (defined by convolving the spectra of the diode output with the absorption band, see Figure 5). The broadening of the absorption line is due to a difference in vibrational coupling of the Yb^{3+} energy levels as well as inhomogeneous broadening. The Yb:Sr_3Ba_2-FAP crystal showed additional absorption features (not shown in the figure) which reduced the overall integrated intensity of the 900 nm absorption band.

In addition, there is a slight shift toward the blue and a change in the ratio of the two peak heights with increasing barium concentration. In Yb:$Sr_{5-x}Ba_x(PO_4)_3F$, the peak at ~900 nm decreases in intensity from x = 0 to x = 5, while the peak at ~895 nm increases until there is a reversal in the dominant peak at concentrations greater than x = 2. This phenomenon is likely due to the atomic site preference of Ba in the fluorapatite structure relative to that of the Yb^{3+} ion. There are two distinct sites for Sr and/or Ba to occupy in the $(A_I)_2(A_{II})_3(PO_4)_3F$ apatite lattice; a larger nine coordinate oxygen site (A_IO_9) and a smaller seven coordinate site containing one fluorine ($A_{II}O_6F$). As Ba is introduced into the lattice, it will preferentially occupy the larger A_IO_9 site altering the vibrational coupling of the Yb^{3+} ion, which prefers the smaller site, thereby broadening the absorption band. This effect continues up to a Ba concentration of x=2 or Yb:Sr_3Ba_2-FAP; for x>2, Ba will begin to occupy the smaller $A_{II}O_6F$ site until x=5, $Ba_5(PO_4)_3F$ (Yb:B-FAP).

The emission spectra plotted in Figure 6 also indicate a moderate reduction in cross section of approximately half for the Ba-containing crystals and inhomogeneous broadening of the peak for crystals with x≥1. The significant decrease in emission cross section with high Ba concentration in the crystals puts restrictions on the preferred stoichiometry of the host lattice to be $0 \leq x \leq 1$, based on laser extraction performance.

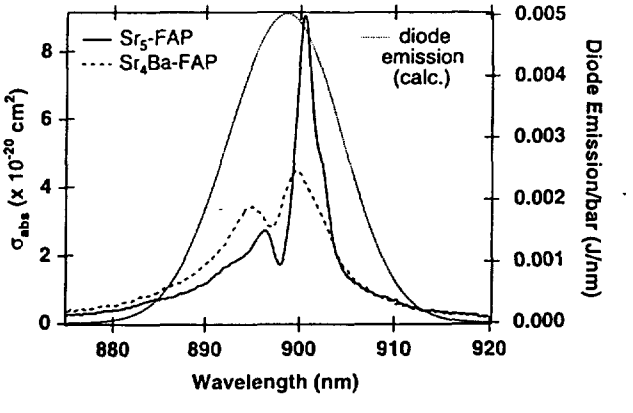

Figure 5. The bandwidth of the absorption spectra of Yb:Sr_4Ba-FAP is compared to that of Yb:S-FAP and a typical pulse width of 8nm for a diode mounted on a BeO heatsink.

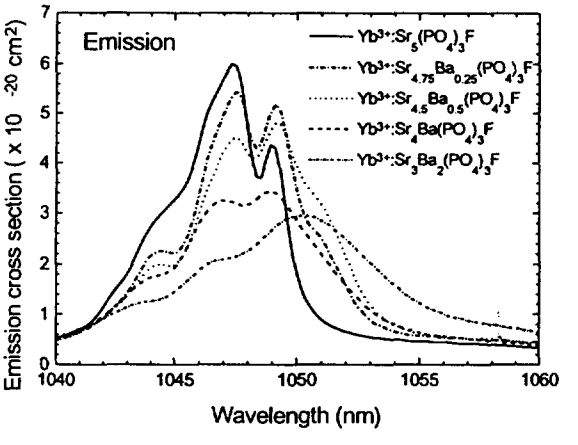

Figure 6. Emission cross sections versus wavelength for Yb:$Sr_{5-x}Ba_x(PO_4)_3F$ crystals.

The Yb^{3+} upper laser level lifetimes are listed in Table I. The lifetime decreases slightly with increasing Ba concentration as might be expected from the broadening of the absorption and emission features suggesting increased asymmetry at the Yb site. In addition, radiation trapping is expected to be an important effect for the Yb-doped apatites as seen for previous experiments performed on Yb:S-FAP where the lifetime increases from 1.10 msec to 1.67 msec for longer pathlength, higher doped crystals.[12] This longer lifetime allows for greater efficiency when using diode pumping.

Table I. Yb^{3+} upper laser level lifetimes.

Material	Intrinsic Lifetime* (msec)
$Sr_5(PO_4)_3F$	1.10
$Sr_{4.75}Ba_{0.25}(PO_4)_3F$	1.13
$Sr_{4.5}Ba_{0.5}(PO_4)_3F$	1.12
$Sr_4Ba(PO_4)_3F$	1.11
$Sr_3Ba_2(PO_4)_3F$	0.98

*low concentration

Gain Experiments and Emission Cross Sections

Small signal gain measurements have been made on crystals 1 cm in thickness, π polarized, with a Cr:LiSAF laser providing pump pulses at 900 nm, and a Nd:YLF laser probing at 1047 nm.[12] A photodiode detector, 1047 nm bandpass filter, and transient digitizer were used to measure the time-dependent gain signals. The gain for a 0.5%Yb:S-FAP crystal was found to be approximately 20% greater when compared to a representative 1.0%Yb:Sr_4Ba-FAP crystal; however, for equal doping levels, the signal is expected to be much larger for Yb:S-FAP (Figure 7).

The emission cross sections of the Ba-containing crystals have been determined by three methods; the method of reciprocity, the Füchtbauer-Ladenburg method, and from small signal gain experiments. The equations describing the calculation of emission cross section from both the Füchtbauer-Ladenburg method and the method of reciprocity have been described elsewhere and will not be repeated here.[3] A simplified equation was used to calculate the emission cross sections from single-pass small signal gain data, $G=\exp[(N_{ex}-\beta N_{gr})\sigma_{em}(\omega_e)2L]$, where N is the number density, β is the branching ratio of the excited state, σ_{em} is the

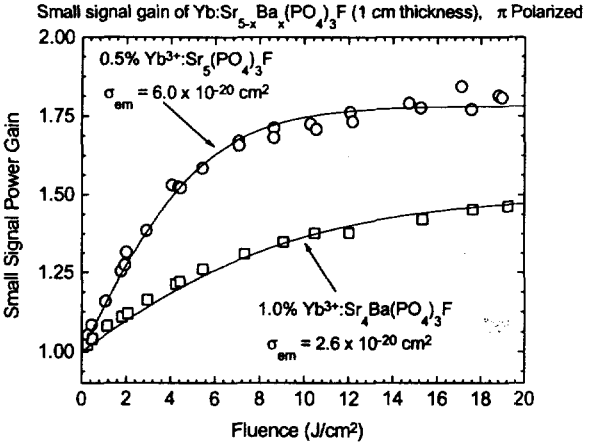

Figure 7. Single-pass small signal gain of Yb:S-FAP and Yb:Sr_4Ba-FAP plotted relative to pump fluence (absorption coefficients for Yb:S-FAP and Yb:Sr_4Ba-FAP are 1.05 cm^{-1} and 0.30 cm^{-1}, respectively).

emission cross section, ω_e describes the pulse shape of the emission band, and L is the length of the crystal. The emission cross sections derived from each of the three methods are reasonably consistent, Table II. A gradual decrease by approximately 50% is seen for Ba concentrations from x=0 to x=1.

Table II. Emission cross sections, derived by three methods, are reasonably consistent.

Material	Emission Cross Section (10^{-20} cm^2)		
	Reciprocity Method	Füchtbauer-Ladenburg Method	Small signal gain Method
Sr_5-FAP	7.0	6.0	6.0
$Sr_{4.75}Ba_{0.25}$-FAP	6.0	5.4	4.7
$Sr_{4.5}Ba_{0.5}$-FAP	5.2	4.8	3.8
Sr_4Ba-FAP	3.8	3.4	2.6
Sr_3Ba_2-FAP	3.3	2.9	--

Summary

The Yb-doped class of apatite crystals offer variable properties for the different needs of various laser applications. In particular, by adding a percentage of Ba into the Yb:S-FAP lattice, the

material and laser parameters can be continuously varied. In particular, the absorption bandwidth increases with Ba concentration to afford more efficient overlap of a diode array pump pulse thereby decreasing the number of diodes necessary for a given laser configuration. However, with this increase in bandwidth there is a continuous decrease in emission cross section by approximately a factor of two from the Yb:S-FAP case. The emission cross sections have been found to be consistent for derived values based on the methods of reciprocity, Füchtbauer-Ladenburg, and small signal gain. Also, the intrinsic laser level lifetime does not appear to change with increasing Ba concentration for Yb:$Sr_{5-x}Ba_x(PO_4)_3F$ crystals. In summary, these materials offer the ability for the laser designer to "dial in" the materials constants for various laser systems rather than jump between different host systems.

Acknowledgment

We would like to express our appreciation to several Lawrence Livermore National Laboratory employees, including H. Powell and W. F. Krupke for their helpful conversations and insight; L. Smith for performing some of the spectroscopic measurements; Jay Skidmore, Mark Emanuel, and Eric Honea for their insight into the output characteristics of laser diode arrays; P. Thelin and R. Vallene for providing the materials fabrication and polishing necessary for samples utilized in optical tests; and T. Duewer for conducting the Yb^{3+} concentration analyses.

References

1. K. Choi and C. A. Wang, "InGaAs/AlGaAs strained single quantum well diode lasers with extremely low threshold current density and high efficiency," Appl. Phys. Lett. Vol. 57, pp. 321-323, 1990.

2. D. P. Bour, G. A. Evans, and D. P. Gilbert, "High-power conversion efficiency in a strained InGaAs/AlGaAs quantum well laser," J. Appl. Phys. Vol. 65, pp. 3340-3343, 1989.

3. L. D. DeLoach, S. A. Payne, L. L. Chase, L.K. Smith, W. L. Kway, and W. F. Krupke, "Evaluation of absorption and emission properties of Yb^{3+} doped crystals for laser applications," IEEE J. Quantum Electron. Vol. 29, pp. 1179-1191, 1993.

4. P. F. Moulton, "Paramagnetic ion lasers," in Handbook of Laser Science and Technology, Vol. I Lasers and Masers, M. Weber, Editor, Florida: CRC Press, Inc. 1982.

5. T. Y. Fan, S. Klunk, and G. Henein, "Diode-pumped Q-switched Yb:YAG laser," Opt. Lett. Vol. 18, pp. 423-425, 1993.

6. K. I. Schaffers, L. D. DeLoach, C. A. Ebbers, and S. A. Payne, "Crystal growth, frequency doubling, and infrared laser performance of Yb^{3+}:$BaCaBO_3F$," IEEE J. Quantum Electron. Vol. 32(5), pp. 741-748, 1996.

7. S. A. Payne, L. D. DeLoach, L. K. Smith, W. L. Kway, and W. F. Krupke, "Ytterbium-doped apatite-structure crystals: A new class of laser materials," J. Appl. Phys. Vol. 76, pp. 497-503, 1994.

8. L. D. DeLoach, S. A. Payne, L. K. Smith, W. L. Kway, and W. F. Krupke, "Laser and spectroscopic properties of $Sr_5(PO_4)_3F$:Yb," J. Opt. Soc. Am. B Vol. 11, pp. 269-276, 1994.

9. C. D. Marshall, L. K. Smith, R. J. Beach, J. A. Emanuel, K. I. Schaffers, J. Skidmore, S. A. Payne, and B. H. T. Chai, "Diode-pumped Ytterbium-doped $Sr_5(PO_4)_3F$ laser performance," IEEE J. Quant. Electron. Vol. 32(4), pp. 650-656, 1996.

10. P. Hong, X. X. Zhang, R. E. Peale, H. Weidner, et. al., "Spectroscopic characteristics of Nd^{3+}-doped strontium fluorovanadate and their relationship to laser performance," J. Appl. Physics, Vol. 77(1), pp. 294-300, 1995. D. Shen, C. Wang, Z. Shao, X. Meng, et. al., "Laser demonstration of diode-laser-pumped neodymium-doped strontium fluorovanadate," Appl. Opt., Vol. 35(12), pp. 2023-2026, 1996.

11. C. D. Marshall, L. K. Smith, S. Sutton, M. A. Emanuel, K. I. Schaffers, S. Mills, S. A. Payne, and W. F. Krupke, in OSA Trends in Optics and Photonics, Advanced Solid-State Lasers, S. A. Payne and C. R. Pollock, Eds., Vol. 1, pp. 208-212, 1996.

12. C. D. Marshall , S. A. Payne, L. K. Smith, H. T. Powell, W. F. Krupke, and B. H. T. Chai, "1.047-μm Yb:$Sr_5(PO_4)_3F$ Energy Storage Optical Amplifier," IEEE J. of Selected Topics in Quantum Electron., Vol. 1(1), pp. 67-77, 1995.

This work was performed under the auspices of the U.S. DOE by LLNL under Contract No. W-7405-ENG-48.

Technical Information Department • **Lawrence Livermore National Laboratory**
University of California • Livermore, California 94551